Analytical Optimization of Low-Frequency Search Coil Magnetometers

Asaf Grosz and Eugene Paperno

***Abstract*— An analytical optimization is proposed for the sensitivity threshold of low-frequency search coil magnetometers employing disk-shape flux concentrators. The optimal diameters of the core and the wire are found for a given set of the optimization parameters: frequency, search coil volume and aspect ratio, relative permeability of the core and the flux concentrators, and the noise of the preamplifier. The proposed analytical optimization allows an immediate analysis of the theoretical limits of the magnetometer sensitivity threshold. An approximation is obtained to simplify and clarify the relationship between the minimum possible sensitivity threshold and the optimization parameters. Measurements performed with an experimental magnetometer model confirm the optimization.**

***Index Terms*— Analytical optimization, disk-shape flux concentrators, low frequency, preamplifier noise, search coil magnetometers, sensitivity threshold.**

NOMENCLATURE

α	Search coil aspect (length to diameter) ratio.
β	Ratio of the wire diameter, including the insulation, and the wire diameter without the insulation: d_{wins}/d_w.
γ	Ratio of the winding length and the total length of the search coil: L_w/L.
μ_r	Relative permeability of the core and the flux concentrators.
μ_a	Apparent permeability of the core.
ρ	Resistivity of the wire.
B	Magnetic field induction.
B_0	Amplitude of the magnetic field induction.
B_{st}	Sensitivity threshold (resolution or equivalent magnetic noise).
$B_{st\,\min}$	Optimum sensitivity threshold (optimum resolution or equivalent magnetic noise).
C	The search coil stray capacitance.
d	Core diameter.
d_{opt}	Optimum core diameter.
d_w	Diameter of the wire, not including the insulation.
$d_{w_{opt}}$	Optimum diameter of the wire, not including the insulation.
d_{wins}	Diameter of the wire, including the insulation.
D	Diameter of the flux concentrators.
e_n	Spectral density of the amplifier voltage noise.
e_R	Spectral density of the coil thermal noise.
e_{tot}	Spectral density of the total coil noise referred to the input.
f	Frequency.
H_D	Demagnetizing factor of a prolate ellipsoid.
i_n	Spectral density of the amplifier current noise.
k	Boltzmann constant.
L	Total length of the search coil, including the flux concentrators.
L_C	The search coil inductance.
L_w	Length of the search coil winding.
N	Number of turns.
R	Search coil winding resistance.
R_{opt}	Search coil winding optimal resistance.
S	Cross-section area of the core.
t	Time.
t_f	Thickness of the flux concentrators.
T	Absolute temperature in kelvin.
$V(f)$	Amplitude of the voltage induced in the search coil by an applied sinusoidal magnetic field.
Vol	Volume of the search coil.

Manuscript received April 5, 2012; accepted May 21, 2012. Date of publication June 1, 2012; date of current version June 13, 2012. This work was supported in part by Analog Devices, Inc., National Instruments, Inc., and the Ivanier Center for Robotics Research and Production Management. The associate editor co-ordinating the review of this paper and approving it for publication was Prof. Bernhard Jakoby.

The authors are with the Department of Electrical and Computer Engineering, Ben-Gurion University of the Negev, Beer-Sheva 84105, Israel (e-mail: paperno@ee.bgu.ac.il; asaf.grosz@gmail.com).

Digital Object Identifier 10.1109/JSEN.2012.2202179

I. INTRODUCTION

LOW-FREQUENCY search coil magnetometers are widely used for geophysical prospecting, space research, magnetic anomaly detection [1]–[17], etc. Their advantages compared to other magnetometers are high resolution and low power consumption, defined only by the power consumption of the preamplifier. The inherent reduction of the search coils' resolution with frequency can be compensated by increasing their size. Thus, large enough low-frequency search coils can compete with and even outperform fluxgates [10]–[12], [16]–[18].

To reach the maximum resolution for a given volume, a search coil magnetometer should be optimized. Conventional approaches to finding the best possible configuration is based on designing the magnetometer part by part [1]–[5]. For example, the search coil core is designed first to provide the maximum apparent permeability, then the coil distribution over the core is selected, and, finally, a preamplifier is developed with low enough noise. To make a search coil more compact, flux concentrators can also be attached to the core [6]–[12].

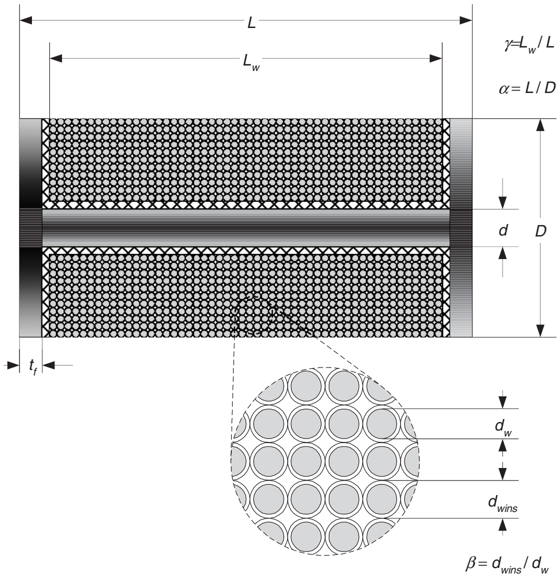

Fig. 1. Search coil structure and dimensions.

Naturally, such a part by part design does not yield the best possible magnetometer configuration.

The optimization of the *entire* magnetometer was suggested in [8]–[13]. This optimization is based on an analytical model that includes the apparent permeability of the core and the flux concentrators, the coil winding, and the noise of the preamplifier. To find the optimum magnetometer configuration for given constraints, for example, for the maximum volume, weight, given power consumption and the noise of the preamplifier, the analytical model is solved numerically for a large set of the parameters, and the configuration providing the best resolution is chosen.

This new approach has advanced the state of the art low-frequency search coil magnetometers by substantially reducing their size, power consumption, and weight for the same resolution [7]–[12].

However, the need to perform a large number of numerical calculations to find the optimum magnetometer configuration makes this approach inconvenient and does not allow one to easily interpret the obtained results: there is no direct, analytical relationship between the magnetometer parameters and its optimal configuration, and, as a result, it is not immediately clear how small changes in the parameters and constraints affect the optimal magnetometer performance.

We overcome this drawback by finding the analytical solutions for the optimum magnetometer parameters. We focus in the present paper only on search coils employing disk-shape flux concentrators (see Fig. 1) and having aspect ratio equal or greater than 2, similar to those described in [9]–[11]. For a given search coil volume and aspect ratio, the relative permeability of the core and the flux concentrators, and the noise of the preamplifier, the optimization of such a magnetometer includes the following five variables: the diameter and thickness of the flux concentrators, the outer diameter of the search coil winding, and the diameters of the core and the wire.

We assume that the diameter of the flux concentrators equals to the maximum diameter of the search coil, as shown in Fig. 1. Employing flux concentrators with maximum possible diameter maximizes the magnetic flux within the core, while practically introducing no noise, and, thus, improves the magnetometer resolution.

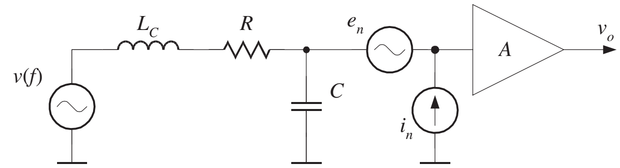

Fig. 2. Equivalent electrical circuit of the search coil magnetometer.

If there are no weight constraints, then in an optimal coil, the entire volume between the flux concentrators, except the core, should be used for winding. Using the maximum possible volume for copper, one can minimize the coil resistance for the same number of turns and, therefore, for the same sensitivity. Minimizing the resistance reduces the coil thermal noise and also the preamplifier noise (see Fig. 2) referred to the input. Thus, the magnetometer sensitivity threshold is improved. Therefore, the external diameter of the winding is always equal to the diameter of the flux concentrators.

Our numerical simulations, performed with Maxwell finite-element software, has shown that increasing the thickness of the flux concentrators beyond 5% of the total length of the search coil does not increase the apparent permeability enough to compensate for the decrease in the magnetometer sensitivity due to the corresponding reduction of the volume of the winding.

Considering the above, we introduce the following assumptions and constraints. (i) We assume that the thickness of the coil bobbin is negligible. (ii) We set the diameter of the flux concentrators equal to the maximum diameter of the search coil. (iii) We set the outer diameter of the winding equal to the diameter of the flux concentrators. (iv) We limit the volume of the search coil, but apply no constrains on its weight, number of turns, and the diameters of the core and wire. (v) We set the thickness of the flux concentrators at 5% of the total length of the search coil ($\gamma = 0.9$).

As a result, the set of the optimization variables includes only the diameters of the core and the wire. We find analytical solutions for these variables assuming that the search coil volume and aspect ratio, the relative permeability of the core and the flux concentrators, and the noise of the preamplifier are given.

The proposed analytical optimization allows an immediate analysis of the theoretical limits of the magnetometer sensitivity threshold as a function of the optimization parameters.

We have also obtained an approximate analytical solution for the minimum possible sensitivity threshold as a function of frequency, the search coil volume and aspect ratio, the preamplifier voltage and current noise product, and the relative permeability of the core and the flux concentrators.

II. Analytical Model of the Magnetometer

The search coil structure and dimensions are shown in Fig. 1 and the equivalent electric circuit of the magnetometer is shown in Fig. 2. The amplitude of the voltage induced in the search coil by an applied sinusoidal magnetic field can be given as follows:

$$V(f) = 2\pi f N S \mu_a B_0 \tag{1}$$

where the number of turns

$$N = \frac{\gamma L}{\beta d_w} \frac{D-d}{2\beta d_w} = \frac{\gamma L(D-d)}{2\beta^2 {d_w}^2} \tag{2}$$

the cross-sectional area of the core

$$S = \frac{\pi \cdot d^2}{4} \tag{3}$$

and the apparent permeability (for $\mu_r >> 1$) [8], [10] and the demagnetizing field [19]

$$\mu_a = \frac{\mu_r}{1+\mu_r \; H_D \; d^2/D^2} \tag{4}$$

$$H_D = \frac{1}{\alpha^2-1}\left[\frac{\alpha}{2\sqrt{\alpha^2-1}}\ln\left(\frac{\alpha+\sqrt{\alpha^2-1}}{\alpha-\sqrt{\alpha^2-1}}\right)-1\right]. \tag{5}$$

At frequencies by an order lower than the search coil self resonance, the search coil inductance and stray capacitance can be neglected, and the spectral density of the total noise of the search coil and the preamplifier (see Fig. 2) referred to the coil input can be given as follows:

$$e_{tot} = \sqrt{e_{R^2} + e_{n^2} + (Ri_n)^2} \tag{6}$$

where

$$e_R = \sqrt{4kTR} \tag{7}$$

and

$$R = N\frac{\pi(D+d)/2}{\pi d_w^2/4}\rho = 2N\frac{D+d}{d_w^2}\rho. \tag{8}$$

At low frequencies, where the search coil reactance can be neglected, the magnetometer sensitivity threshold can be defined as $B_{st}(f)$ for which the induced voltage (1) equals the spectral density of the total noise (6):

$$B_{st}(f) = \frac{\sqrt{e_R^2 + e_n^2 + (Ri_n)^2}}{2\pi f N S \mu_a}. \tag{9}$$

III. Analytical Optimization of the Magnetometer

The optimization goal is to find the optimum diameter of the core and the wire, d_{opt} and d_{wopt}, that minimize $B_{st}(f)$ for a given frequency, f, volume, Vol, and aspect ratio, α, of the search coil, relative permeability of the core and the flux concentrators material, μ_r, and the preamplifier's equivalent noise: e_n and i_n.

To find d_{opt} and d_{wopt}, we solve the system of equations defining the minimum of the magnetometer sensitivity threshold:

$$\begin{cases} \frac{\partial B_{st}(f)}{\partial d} = 0 \\ \frac{\partial B_{st}(f)}{\partial d_w} = 0. \end{cases} \tag{10}$$

The only real and positive solutions of (10) are:

$$d_{opt} = \frac{1}{3\mu_r H_D}\left[\frac{D^2(4-3\mu_r H_D)}{\sqrt[3]{A}} + \sqrt[3]{A} - 2D\right] \tag{11}$$

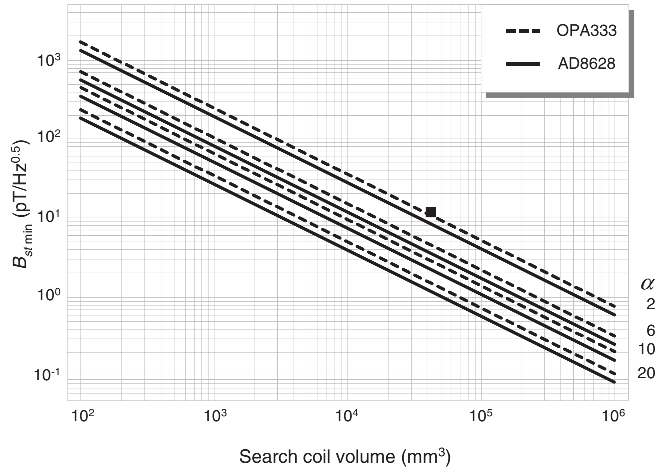

Fig. 3. Minimum sensitivity threshold as a function of the search coil volume and aspect ratio, and the noise of the preamplifier. The equivalent noise of the preamplifiers is: 15 nV/$\sqrt{}$Hz and 5 fA/$\sqrt{}$Hz for the AD8628 and 55 nV/$\sqrt{}$Hz and 100 fA/$\sqrt{}$Hz for the OPA333. $\mu_r = 2000$, $f = 1$ Hz, $\rho = 1.678 \times 10^{-8}$, $\beta = 1.15$, $\gamma = 0.9$, and $T = 300$ K. The experimental data (see Table I) is shown by the square mark.

where

$$A = D^3[9\mu_r H_D(1+3\mu_r H_D) - 8] + \sqrt{27}\sqrt{D^6(\mu_r H_D)^2[\mu_r H_D(19+27\mu_r H_D)-17]} \tag{12}$$

and

$$d_{wopt} = \sqrt[4]{\frac{\gamma L(D^2 - d_{opt}^2) i_n \rho}{\beta^2 e_n}}. \tag{13}$$

It is interesting to note that according to (2), (8) and (13), the coil winding optimal resistance depends only on the noise parameters of the amplifier:

$$R_{opt} = \frac{e_n}{i_n}. \tag{14}$$

To illustrate the above theory, we plot in Fig. 3 the minimum possible sensitivity threshold, $B_{stmin}(f)$, as a function of the search coil volume and aspect ratio, and the preamplifier noise. $B_{stmin}(f)$ in Fig. 3 is found according to (1)-(9), where d and d_w are substituted with their optimum values, d_{opt} and d_{wopt}, according to (11), (12) and (13), respectively.

The optimum core and wire diameters are sown in Figs. 4 and 5, respectively, as a function of the search coil volume and aspect ratio. The optimum wire diameter also depends on the noise of the preamplifier.

To simplify and clarify the relationship between $B_{stmin}(f)$ and the optimization parameters, it can be approximated as follows:

$$B_{st\,\min}(f) \approx 3.65 \times 10^{-4}\sqrt{8.28 \times 10^{-21} + e_n i_n} \times (\alpha Vol)^{-0.833}\left(7.64 \times 10^{-2} + \mu_r^{-0.449}\right) f^{-1} \tag{15}$$

where B_{stmin}(f) is in the units of T/$\sqrt{}$Hz, f is in the units of Hz, e_n and i_n are in the units of V/$\sqrt{}$Hz and A/$\sqrt{}$Hz, respectively, and Vol is in the units of m^3.

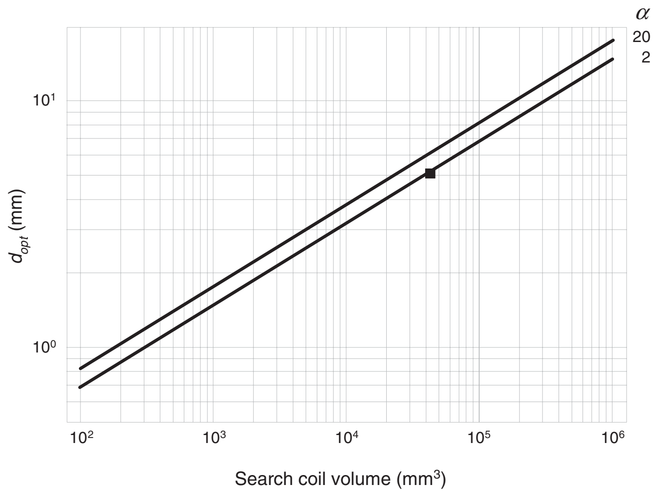

Fig. 4. Optimum diameter of the core as a function of the search coil volume and aspect ratio. $\mu_r = 2000$, $f = 1$ Hz, $\rho = 1.678 \times 10^{-8}$, $\beta = 1.15$, $\gamma = 0.9$, and $T = 300$ K. The experimental data (see Table I) is shown by the square mark.

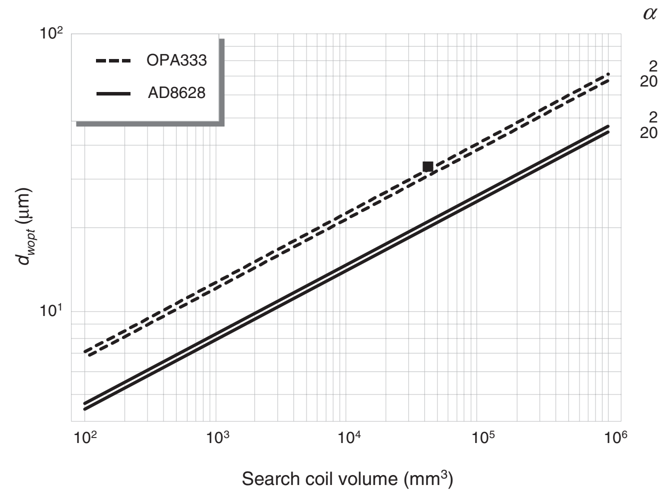

Fig. 5. Optimum diameter of the wire as a function of the search coil volume and aspect ratio, and the noise of the preamplifier. The equivalent noise of the preamplifiers is: 15 nV/$\sqrt{\text{Hz}}$ and 5 fA/$\sqrt{\text{Hz}}$ for the AD8628 and 55 nV/$\sqrt{\text{Hz}}$ and 100 fA/$\sqrt{\text{Hz}}$ for the OPA333. $\mu_r = 2000$, $f = 1$ Hz, $\rho = 1.678 \times 10^{-8}$, $\beta = 1.15$, $\gamma = 0.9$, and $T = 300$ K. The experimental data (see Table I) is shown by the square mark.

TABLE I
PARAMETER OF THE MAGNETOMETER

Parameters	Theoretical model	Experimental model
Constrains		
L	60 mm	60 mm
L_w	54 mm	52 mm
D	30 mm	30 mm
Vol	42411 mm^3	42411 mm^3
α	2	2
β	1.15	1.14
γ	0.9	0.87
μ_r	2000	2000
e_n	55 nV/$\sqrt{\text{Hz}}$	55 nV/$\sqrt{\text{Hz}}$
i_n	100 fA/$\sqrt{\text{Hz}}$	100 fA/$\sqrt{\text{Hz}}$
t_f	3 mm	3 mm
Optimal parameters		
d_{opt}	5.16 mm	5 mm
d_{wopt}	32.3 μm	35 μm
Sensitivity threshold		
B_{stmin}	10.86 pT/$\sqrt{\text{Hz}}$	11.2 pT/$\sqrt{\text{Hz}}$

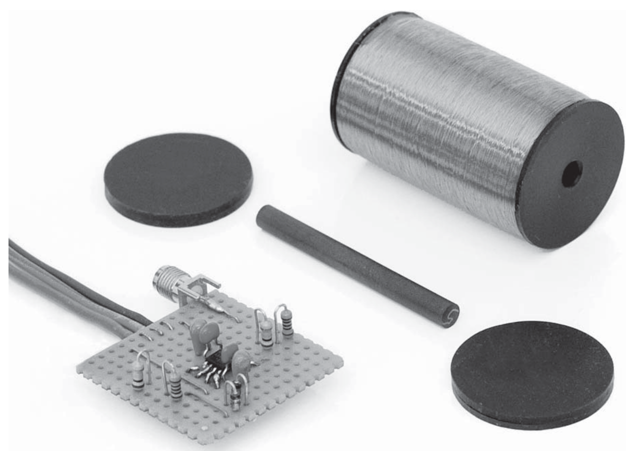

Fig. 6. Magnetometer components.

The inaccuracy of approximation (15) compared to the exact analytical optimization is less than 37% for $2<\alpha<20$, $200<\mu_r<20\times10^3$, 0.1 nV/$\sqrt{\text{Hz}}$ $< e_n <$ 10 μV/$\sqrt{\text{Hz}}$, 0.1 fA/$\sqrt{\text{Hz}}$ $< i_n <$10 pA/$\sqrt{\text{Hz}}$, 10^{-6} m^3 $< Vol <$1 m^3. For $10^3 < \mu_r < 5\times10^3$, the inaccuracy is less than 21%.

It is important to note from (15) that any preamplifier with the $e_n i_n$ product much smaller than 8.28×10^{-21} has negligible effect on the magnetometer sensitivity threshold.

Approximation (15) has been obtained for T = 300 K and for copper wire ($\rho = 1.678\times10^{-8}$) with thin isolation, $\beta = 1.15$.

IV. Experiment

To verify the theoretical sensitivity threshold $B_{stmin}(f)$ obtained in Fig. 3 in accordance with (1)-(9) and (11)-(13), we built and tested an experimental model of the search coil magnetometer. The magnetometer components are shown in Fig. 6, and its parameters are listed in Table I.

Table I represents a comparison between the experimental and theoretical models. The optimal parameters of the core and wire for the theoretical model were calculated for a set of given parameters (the constrains in Table I). The parameters of the experimental model were chosen as close as possible to the parameters of the theoretical model.

Our measurements show that the experimental value of B_{stmin} at 1 Hz (11.2 pT/$\sqrt{\text{Hz}}$) is very close to the theoretical one (10.86 pT/$\sqrt{\text{Hz}}$).

V. Conclusion

Analytical solutions for the optimum parameters of low-frequency search coil magnetometers has been obtained for the first time, to the best of our knowledge. To obtain the analytical solution for the optimal sensitivity threshold, $B_{stmin}(f)$, for a given frequency, f, volume, Vol, aspect ratio, α, relative permeability of the core and the flux concentrators material, μ_r, and the preamplifier noise, e_n and i_n, we applied the constraints described in the Introduction and, by using equations (1)-(8), reduced the number of $B_{min}(f)$ variables in (9) to only two: d and d_w. We then found d_{opt} and d_{wopt} that minimize $B_{st}(f)$. $B_{stmin}(f)$ represents the theoretical limit of the magnetometer sensitivity threshold.

To simplify and clarify the relationship between $B_{stmin}(f)$, the noise parameters of the preamplifier, e_n and i_n, the search coil aspect ratio, α, relative permeability of the core and the flux concentrators material, μ_r, and its volume, *Vol*, we have obtained approximation (15). Based on (15), a criterion for neglecting the preamplifier noise is formulated: $e_n i_n << 8.28\times10^{-21}$. It is also immediately clear from (15), what the impact is of the preamplifier noise on $B_{stmin}(f)$.

The developed theory helps the designer to immediately find the best possible sensitivity threshold and the optimal parameters of a search coil for a given volume, aspect ratio, preamplifier and relative permeability of the core and the flux concentrators material.

We have used in our analysis two different, commercially available zero-drift amplifiers with no flicker noise. One of these amplifiers, the AD8628, has low enough noise to be regarded as an almost ideal preamplifier since it increases the sensitivity threshold only by about 0.5%. On the other hand, the current consumption of the AD8628 is relatively high (850 μA). The OPA333 preamplifier has a 50 times lower current consumption (17 μA) but a higher noise. However, the sensitivity threshold degradation caused by the OPA333 is only about 30%.

Measurements performed with an experimental magnetometer model confirm the optimization.

References

[1] P. Ripka, *Magnetic Sensors and Magnetometers*. Boston, MA: Artech House, 2000.

[2] H. C. Séran and P. Fergeau, “An optimized low-frequency three-axis search coil magnetometer for space research,” *Rev. Sci. Instrum.*, vol. 76, no. 4, pp. 044502-1–044502-10, 2005.

[3] R. J. Prance, T. D. Clark, and H. Prance, “Compact broadband gradiometric induction magnetometer system,” *Sensors Actuat. A, Phys.*, vol. 76, nos. 1–3, pp. 117–121, Aug. 1999.

[4] R. J. Prance, T. D. Clark, and H. Prance, “Compact room-temperature induction magnetometer with superconducting quantum interference device level field sensitivity,” *Rev. Sci. Instrum.*, vol. 74, no. 8, pp. 3735–3739, 2003.

[5] R. J. Prance, T. D. Clark, and H. Prance, “Ultralow noise induction magnetometer for variable temperature operation,” *Sensors Actuat. A, Phys.*, vol. 85, nos. 1–3, pp. 361–364, 2000.

[6] K. Abe and J. I. Takada, “Simulation and design of a very small magnetic core loop antenna for an LF receiver,” *IEICE Trans. Commun.*, vol. E90-B, no. 1, pp. 122–130, Jan. 2007.

[7] Z. Chen, S. Zhou, and A. Jiang, “Miniaturization design on magnetic induction sensors,” in *Proc. Int. Conf. Electron. Mech. Eng. Inf. Technol.*, Aug. 2011, pp. 4626–4629.

[8] C. Coillot, J. Moutoussamy, R. Lebourgeois, S. Ruocco, and G. Chanteur, “Principle and performance of a dual-band search coil magnetometer: A new instrument to investigate fluctuating magnetic fields in space,” *IEEE Sensors J.*, vol. 10, no. 2, pp. 255–260, Feb. 2010.

[9] C. Coillot, J. Moutoussamy, G. Chanteur, and A. Roux, “Improvements on the design of search coil magnetometer for space experiments,” *Sensor Lett.*, vol. 5, no. 1, pp. 167–170, 2007.

[10] E. Paperno and A. Grosz, “A miniature and ultralow power search coil optimized for a 20 mHz to 2 kHz frequency range,” *J. Appl. Phys.*, vol. 105, no. 7, pp. 07E708-1–07E710-3, Apr. 2009.

[11] A. Grosz, E. Paperno, S. Amrusi, and E. Liverts, “Integration of the electronics and batteries inside the hollow core of a search coil,” *J. Appl. Phys.*, vol. 107, no. 9, pp. 09E703-1–09E703-3, 2010.

[12] A. Grosz, E. Paperno, S. Amrusi, and B. Zadov, “A three-axial search coil magnetometer optimized for small size, low power, and low frequencies,” *IEEE Sensors J.*, vol. 11, no. 4, pp. 1088–1094, Apr. 2011.

[13] D. G. Lukoschus, “Optimization theory for induction-coil magnetometers at higher frequencies,” *IEEE Trans. Geosci. Electron.*, vol. 17, no. 3, pp. 56–63, Jul. 1979.

[14] A. Grosz, E. Paperno, S. Amrusi, and T. Szpruch, “Minimizing crosstalk in three-axial induction magnetometers,” *Rev. Sci. Instrum.*, vol. 81, no. 12, pp. 125106-1–125106-9, 2010.

[15] E. Paperno, A. Grosz, S. Amrusi, and B. Zadov, “Compensation of crosstalk in three-axial induction magnetometers,” *IEEE Trans. Instrum. Meas.*, vol. 60, no. 10, pp. 3416–3422, Oct. 2011.

[16] *Magnetic Field Induction Sensor BF-7*. (2012) [Online]. Available: http://www.slb.com/~/media/Files/rd/technology/product_sheets/emi_bf_7_sensor.ashx

[17] *Broad Band Induction Coil Magnetometer MFS-06e*. (2012) [Online]. Available: http://178.63.62.205/mtxgeo/index.php/sensors/mfs-06e

[18] *Induction Magnetometer for Geophysical Applications LEMI-121*. (2012) [Online]. Available: http://www.isr.lviv.ua/lemi121.htm

[19] J. A. Osborn, “Demagnetizing factors of the general ellipsoid,” *Phys. Rev.*, vol. 67, nos. 11–12, pp. 351–357, 1945.

Asaf Grosz received the B.Sc. degree in physics and computer science from Tel-Aviv University, Tel-Aviv, Israel, in 2007. He is currently pursuing the M.Sc. degree with the Department of Electrical and Computer Engineering, Ben-Gurion University of the Negev, Beer-Sheva, Israel.

His current research interests include magnetometry, magnetic sensors, low-noise, and ultra-low-power electronics.

Eugene Paperno received the B.Sc. and M.Sc. degrees in electrical engineering from the Minsk Institute of Radio Engineering, Minsk, Belarus, in 1983, and the Ph.D. degree (*summa cum laude*) from the Ben-Gurion University of the Negev, Beer-Sheva, Israel, in 1997.

He was with the Institute of Electronics, Belorussian Academy of Sciences, Minsk, from 1983 to 1991. From 1997 to 1999, he was a Japan Society for the Promotion of Science Post-Doctoral Fellow with Kyushu University, Fukoka, Japan. Since 1999, he has been with the Department of Electrical and Computer Engineering, Ben-Gurion University of the Negev. His current research interests include magnetic sensors, including atomic magnetometers, magnetic shielding, magnetic tracking, and magnetic and electronic instrumentation.